19th International Conference on
Adaptive Structures and Technologies
October 6-9, 2008
Ascona, Switzerland

Maximizing the Excitation Strength at Specific Resonance Frequencies of Functionally Graded Piezoelectric Transducers

Wilfredo Montealegre Rubio[1]*, Emílio Carlos Nelli Silva[2]
[1 2]Department of Mechatronics and Mechanical Systems Engineering, University of São Paulo,
Av. Prof. Mello Moraes, 2231 - Cidade Universitária, São Paulo – SP, CEP: 05508-900, Brazil
[1]wilfredo.rubio@poli.usp.br; [2]ecnsilva@usp.br

ABSTRACT

An important parameter in piezoelectric transducer design is to maximize the strength of a specific resonance when a voltage is applied across the electrodes. In this work, it is proposed a new approach to design piezoelectric transducer based on the maximization of the excitation strength of user-defined modes. Here, the piezoelectric transducer is designed based on Functionally Graded Material (FGM) concept (named Functionally Graded Piezoelectric Transducers (FGPT)). FGM are composite advanced materials, which are made by changing gradually the properties with position inside material domain. In this work, Topology Optimization Method (TOM) is applied to find the optimal gradation function that maximizes the excitation strength of desirable modes. The Piezoelectric Modal Constant (PMC) is considered to quantify the excitation strength of a specific mode. The main goal is to maximize a specified PMC of a specific FGPT mode by finding the optimal material distribution subjected to a given volume constraint. In addition, the FGPT is required to oscillate in a thickness extensional mode (aiming acoustic wave generation applications); thus, to track the desirable mode a mode-tracking method based on the Modal Assurance Criterion (MAC) is applied. The optimization algorithm is constructed based on Sequential Linear Programming (SLP), and the concept of the Continuum Approximation of Material Distribution (CAMD) is considered. To illustrate the method, two-dimensional FGPT are designed considering plane strain assumption. The result shows the advantage of using FGM concept and TOM to design piezoelectric transducers. The desired PMC is increased more than 60%. In addition, the target mode is achieved by using an accurate mode-tracking strategy.

Keywords: Piezoelectric Transducers, FGM, Topology Optimization Method, Piezoelectric Modal Constant, Mode-Tracking.

1. INTRODUCTION

Piezoelectric materials are multifunctional materials; they have the property to convert electrical energy (electric field and electric potential) into mechanical energy (stress and strain) and vice-versa. Nowadays, a new concept has been applied to design piezoelectric transducer: Functionally Graded Material (FGM) concept. In this work, these piezoelectric transducers are named Functionally Graded Piezoelectric Transducers (FGPT). FGM posses continuous graded properties with gradual change in microstructure [1]. In piezoelectric transducer design the FGM concept can be applied for improving their performance: as reduction of stress concentration [2], increasing bonding strength and fatigue-lifetime [3]. In addition, the FGM concept allows designing

of piezoelectric transducers with smaller time waveform (large bandwidth) [4], which is desired in medical imaging and non-destructive testing (NDT) applications. Basically, in FGPT all its properties (dielectric, elastic and piezoelectric constants) or some of them vary along a specific direction, as shown in Fig.1, usually along its thickness, based on several gradation functions.

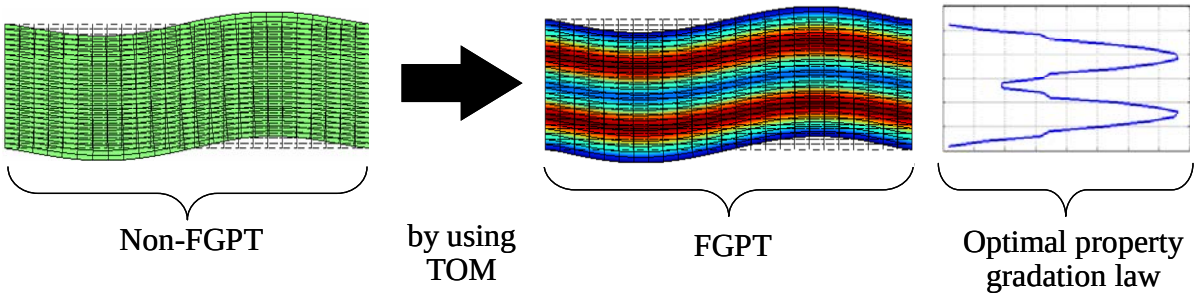

Figure 1. Functionally Graded Piezoelectric Transducer principle.

FGPT design can be divided, mainly, into analytical and finite element approaches. Analytical issues mainly deals with applications of analytical techniques which, usually, grade a unique material property of the FGPT, for instance, the elastic constant c_{11} [5]; or the piezoelectric constant d_{31} [6]. Other papers elucidating analytical modeling of free and forced vibrations are the works of Yang and Xiang [7] and Zhong and Yu [8]. These analytical approaches are limited to simulate two-dimensional piezoelectric structures and to simulate the FGPT behavior when two or more material properties are graded. On the contrary, by using finite element approaches, 2D and/or 3D FGPT considering several gradation functions at one or more properties can be designed; however, these numerical approaches are based on multilayer design, where for each lamina of multilayer piezoceramic the material properties are uniform, smoothly changing among layers [9]. Moreover, the multilayer approach is not accurate enough for calculating stresses and dynamic behavior, since the stress concentration among layers is increased, and the result is depended of layer number utilized. In order to reduce that trouble, the material gradation is treated based on Graded Finite Element (GFE) concept [10], which incorporates the material property gradient at the size scale of the finite element, resulting in smooth and accurate change of properties among GFE. Nowadays, a novel approach has been utilized: design of FGPT based on Topology Optimization Method (TOM) [11], but considering only static analysis. That quasi-static design does not involve several important problems that arise in dynamic operations; specifically, it does not deal with eigenmode switching during the optimization process; non-smooth objective functions; and discontinuous sensitivities of the objective function

In view of above ideas, this research proposes a new, generic and systematic Topology Optimization formulation to find the optimum material gradation of FGPT, see Fig. 1, in order to modify the dynamic characteristics of FGPT and to achieve the following goals: to maximize the excitation strength of selective vibration mode shapes and, to design FGPT with desired mode shapes. Tracking a desirable eigenmode is particularly useful in acoustic wave generation applications, since the FGPT is required to oscillate in thickness extensional mode or piston-like mode [12]. To achieve these goals, a MATLAB code is implemented, which includes mode-tracking method for tracking the target eigenmode; specifically, the Modal Assurance Criterion (MAC) is applied [13]. To treat the material gradation, the Graded Finite Element (GFE) formulation is implemented [10]. The optimization algorithm is constructed based on Sequential Linear Programming (SLP), and the concept of the Continuum Approximation of Material Distribution (CAMD) is considered [14] for modelling a continuous distribution of material along the design domain instead of the traditional piecewise material distribution applied by traditional topology optimization formulation [15]. In addition, to achieve an explicit gradient control, design variable projection [16] is implemented.

2. FINITE ELEMENT MODELING OF FGPT

The well-known matrix formulation of the equilibrium equations for a piezoelectric medium is formulated, without structural damping, as [17]:

$$\begin{bmatrix} \boldsymbol{M_{uu}}(x,y) & 0 \\ 0 & 0 \end{bmatrix} \begin{Bmatrix} \ddot{\boldsymbol{U}} \\ \ddot{\boldsymbol{\varphi}} \end{Bmatrix} + \begin{bmatrix} \boldsymbol{K_{uu}}(x,y) & \boldsymbol{K_{u\varphi}}(x,y) \\ \boldsymbol{K_{u\varphi}}(x,y) & -\boldsymbol{K_{\varphi\varphi}}(x,y) \end{bmatrix} \begin{Bmatrix} \boldsymbol{U} \\ \boldsymbol{\varphi} \end{Bmatrix} = \begin{Bmatrix} \boldsymbol{F} \\ \boldsymbol{Q} \end{Bmatrix} \tag{1}$$

where $\boldsymbol{U}$ is the nodal displacement vector; $\boldsymbol{\varphi}$ is the nodal electric potential vector; $\boldsymbol{F}$ and $\boldsymbol{Q}$ are the nodal mechanical force and electric charge vectors, respectively. $\boldsymbol{M_{uu}}$, $\boldsymbol{K_{uu}}$, $\boldsymbol{K_{u\varphi}}$, and $\boldsymbol{K_{\varphi\varphi}}$ are respectively the mass, elastic, piezoelectric and dielectric "stiffness" matrices. However, when a FGPT is considered, the properties change continuously inside the piezoelectric domain, which means that the matrices of eq. (1) must be described by some continuous function of Cartesian position (x, y) into a bi-dimensional FGPT. Hence, the matrices of Eq. (1) are expressed as:

$$\begin{aligned} &\boldsymbol{M_{uu}}(x,y) = \iint \boldsymbol{N_u}^T \rho(x,y) \boldsymbol{N_u}\, dx\, dy; \quad \boldsymbol{K_{uu}}(x,y) = \iint \boldsymbol{B_u}^T \boldsymbol{C}^E(x,y) \boldsymbol{B_u} dx\, dy; \\ &\boldsymbol{K_{u\varphi}}(x,y) = \iint \boldsymbol{B_u}^T \boldsymbol{e}^T(x,y) \boldsymbol{B_\varphi} dx\, dy; \quad \boldsymbol{K_{\varphi\varphi}}(x,y) = \iint \boldsymbol{B_\varphi}^T \varepsilon^S(x,y) \boldsymbol{B_\varphi} dx\, dy \end{aligned} \tag{2}$$

where, $\boldsymbol{N_u}$ are the shape functions for the displacements; and $\boldsymbol{B_u}$ and $\boldsymbol{B_\varphi}$ are the strain-displacement and voltage-gradient matrices, respectively. $\boldsymbol{C^E}$, $\boldsymbol{e}$, and $\boldsymbol{\varepsilon^S}$ respectively represent the elastic, piezoelectric, and dielectric material constants. According to the theory of conventional finite element, the matrices and vectors of piezoelectric constitutive equations result from assembling the vectors and matrices of the single elements [17].

In modal analysis, the eigenvalues and eigenmodes are found solving the second-order systems:

$$-\lambda \begin{bmatrix} \boldsymbol{M_{uu}}(x,y) & \boldsymbol{0} \\ \boldsymbol{0} & \boldsymbol{0} \end{bmatrix} \begin{Bmatrix} \boldsymbol{\Psi_u} \\ \boldsymbol{\Psi_\varphi} \end{Bmatrix} + \begin{bmatrix} \boldsymbol{K_{uu}}(x,y) & \boldsymbol{K_{u\varphi}}(x,y) \\ \boldsymbol{K_{u\varphi}}^T(x,y) & -\boldsymbol{K_{\varphi\varphi}}(x,y) \end{bmatrix} \begin{Bmatrix} \boldsymbol{\Psi_u} \\ \boldsymbol{\Psi_\varphi} \end{Bmatrix} = \begin{Bmatrix} \boldsymbol{0} \\ \boldsymbol{0} \end{Bmatrix} \quad \text{with} \quad \lambda = \omega^2 \tag{3}$$

where, λ and ω are respectively the eigenvalue and natural frequency, and $\{\boldsymbol{\Psi}\} = \{\boldsymbol{\Psi_u}, \boldsymbol{\Psi_\varphi}\}^T$ represents the eigemode vector.

2-1. Piezoelectric Modal Constant (PMC)

The Piezoelectric Modal Constant (PMC) determines, for a specific vibrating mode, how strong the couple is between the mode and the excitation; in other words, the PMC determines the relative importance of a specific vibrating mode [12]. Accordingly, if it wants to increase the contribution of a specific mode, its PMC must be increased. The piezoelectric modal constant A_{r_k} depends on eigenmode $\boldsymbol{\Psi}_{r_k}$ of mode k, and it is formulated as [12]:

$$A_{r_k} = W_{r_k}^2 \quad \text{with:} \quad W_{r_k} = \{\boldsymbol{\Psi}_{r_k}\}^T \{\boldsymbol{W}_F\} \tag{4}$$

where $\boldsymbol{W}_F$ is the equivalent nodal force vector that converts the applied voltage on electrodes to a mechanical force at each finite element node. The equivalent nodal vector is given by [12]:

$$\{\boldsymbol{W}_F\} = \begin{bmatrix} \boldsymbol{K_{u\varphi_p}} \\ \boldsymbol{K_{\varphi_i\varphi_p}} \end{bmatrix} \{\boldsymbol{I}_p\} \tag{5}$$

where $\boldsymbol{I}_p$ is a vector with length equal to the number of nodes on the electrode with varying potential (ungrounded electrode), and where the matrix $\left\lfloor \boldsymbol{K}_{u\varphi_p} \quad \boldsymbol{K}_{\varphi_i\varphi_p} \right\rfloor^T$ results to transform the Eq. (3) into a FE equation where the nodes are condensed out in electroded nodes and non-electroded nodes. Thus, for a TPGF exited by a voltage applied between a grounded electrode on its bottom surface and an ungrounded electrode on its top surface, the subscripts *i* and *p* denote respectively the electrical potential degree freedom of the non-electroded nodes and ungrounded electroded nodes. $\boldsymbol{K}_{u\varphi_p}$ and $\boldsymbol{K}_{\varphi_i\varphi_p}$ are corresponding coupling stiffness matrices.

3. TOM FORMULATION FOR DESIGNING FGPT

The objective function consists to maximize the PMC (A_r) of a specified mode or set of modes. As mentioned in section 2, the PMC is important since it evaluates how strong the excitation of a specific mode is in the transducer response. That objective function is given by:

$$F = \left[\frac{1}{\alpha} \left(\sum_{k=1}^{m} w_k \left(A_{r_k} \right)^n \right) \right]^{1/n} \quad \text{with} \quad \alpha = \sum_{k=1}^{m} w_k \; ; \quad n = -1, -3, -5, -7... \tag{6}$$

where A_{r_k} and w_k are respectively the PMC and weight coefficients for mode k (k = 1, 2,…, m), m is the number of modes considered in the multi-objective function, and n is a given power.

The optimization problem is formulated as to find the material gradation of FGPT which maximizes the multi-objective function F subjected to piezoelectric volume constraint. That constraint is implemented to control the amount of piezoelectric material into the design domain, Ω. Hence, the optimization problem is given as:

$$\begin{aligned} &\underset{\rho_{TOM}(x,y)}{maximize} && \left[\frac{1}{\alpha} \left(\sum_{k=1}^{m} w_k \left(A_{r_k} \right)^n \right) \right]^{1/n} \; ; \quad \alpha = \sum_{k=1}^{m} w_k \; ; \quad n = -1, -3, -5, -7... \\ &\textit{subjected to :} && \int_{\Omega} \rho_{TOM}(x,y) d\Omega - \Omega_s \leq 0 \\ & && 0 \leq \rho_{TOM}(x,y) \leq 1 \\ & && \textit{Equilibrium equation, see Eq.(3)} \end{aligned} \tag{7}$$

where $\rho_{TOM}(x, y)$ is the design variable (pseudo-density) at Cartesian coordinates x and y. Ω_s describes the amount of material *type 1*, see Eq.(5), at bi-dimensional domain Ω. The second requirement (mode shape tracking) is achieved by using the Modal Assurance Criterion (MAC) [13], which is widely used to compare experimental modal analysis with theoretical one. Since FGPR can be constructed by sintering a layer-structured ceramic green body without using adhesive material, the optimization problem is arranged as a like-layer optimization problem; in other words, the design variables are considered equals at each interfacial layer. This like-layer makes the FGPR manufacturing possible. However, the like-layer optimization implies that the finite element mesh must be homogeneous.

The adopted material model is based on a simple extension of the traditional SIMP model [15]:

$$E^H(x,y) = \rho_{TOM}(x,y) E_1(x,y) + (1 - \rho_{TOM}(x,y)) E_2(x,y) \tag{8}$$

where E^H denotes the mixture material properties. The tensor E_i is related to the stiffness or piezoelectric or dielectric properties for material *type i* (i = 1, 2). ρ_{TOM} = 1.0 denotes material properties *type 1*, and ρ_{TOM} = 0.0 denotes material properties *type 2*, both at Cartesian coordinates x and y. Material *type 1* and *type2* depict the fundamental material properties to be "mixed".

4. NUMERICAL IMPLEMENTATION

4-1. Continuous gradation of material properties and design variables

To treat the gradation in FGPT, the material property is continuously interpolated inside each finite element based on property values at each finite element node. This approach is named Graded Finite Element (GFE) formulation [10]. In this research, the piezoelectric GFE employs the same shape functions N to interpolate the unknown nodal displacements and electrical potentials, spatial coordinates, and the material constants. Thus, the elastic, C^E, piezoelectric, e, and dielectric, ε^S, material constants, in Eq.(2), are respectively given by:

$$\begin{aligned} &C^E_{ijkl}(x,y)=\sum_{n=1}^{m} N_n(x,y)\left(C^E_{ijkl}\right)_n, \quad e_{ikl}(x,y)=\sum_{n=1}^{m} N_n(x,y)\left(e_{ikl}\right)_n, \quad \textit{and} \\ &\varepsilon^S_{ik}(x,y)=\sum_{n=1}^{m} N_n(x,y)\left(\varepsilon^S_{ik}\right)_n \qquad \textit{for} \quad i,j,k,l=1,2,3 \end{aligned} \tag{9}$$

where m is the number of nodes per finite element.

On the other hand, the Continuum Approximation of Material Distribution (CAMD) concept [14] is used to continuously represent the material distribution. CAMD considers that the design variables inside of the finite element are interpolated by using, for instance, the FE shape functions, N. Thus, the pseudo-density ρ^e_{TOM} at each graded finite element e can be expressed as:

$$\rho^e_{TOM}(x,y)=\sum_{i=1}^{n_d} \rho^n_{TOM_i} N_i(x,y) \tag{10}$$

where $\rho^n_{TOM_i}$ and N_i are respectively the nodal design variable and shape function for node i (i = 1,…n_d), and n_d is the number of nodes at each GFE. This formulation allows to have a continuous distribution of material along the design domain instead of the traditional piecewise material distribution applied by previous formulation of topology optimization [15].

Finally, a new scheme to achieve an explicitly gradient control is implemented by introducing a layer of nodal variables on top of the existing nodal variables [16]. The variables in the new layer are used as design variables, which are update by the iterative optimization process. The projection technique employs a function to relate the nodal design variable $\rho^n_{TOM_i}$ to the nodal material density $\rho^p_{TOM_i}$. That projection function is defined as:

$$\rho^P_{TOM_i}=f\left(\rho^n_{TOM_j}\right)=\frac{\sum_{j\in S_i}\rho^n_{TOM_j} W(r_{ij})}{\sum_{j\in S_i} W(r_{ij})} \quad \text{with} \quad r_{ij}=\|\mathbf{x}_j-\mathbf{x}_i\| \tag{11}$$

where $\rho^n_{TOM_i}$ is the nodal design variable assumed to be located at node i; $\rho^p_{TOM_j}$ is the material density

located at node j; and S_i is the set of nodes j in the sub-domain under influence of node i. In other words, the sub-domain S_i corresponds to a circle with its center located at the node i and user-defined radius equal to r_{min}. $\boldsymbol{x}_i$ and $\boldsymbol{x}_j$ represent the Cartesian coordinate of node i and j, respectively. Lastly, W represents a weight function [16].

4-2. Modal Assurance Criterion (MAC)

The Modal Assurance Criterion (MAC) is implemented to track the desirable mode shape [18]. In topology optimization, MAC was initially implemented to maximize eigenvalues associated with specified target modes of non-piezoelectric structures [13]. In this work, MAC is utilized to compare the user-defined or target eigenmode shape, $\boldsymbol{\Psi}_{ref}$, with the current eigenmode shape, $\boldsymbol{\Psi}_c$, obtained from topology optimization process. MAC is defined as [13,18]:

$$\mathrm{MAC}\left(\boldsymbol{\Psi}_{ref},\boldsymbol{\Psi}_c\right)=\frac{\left|\boldsymbol{\Psi}_{ref}^T\boldsymbol{\Psi}_c\right|^2}{\left(\boldsymbol{\Psi}_{ref}^T\boldsymbol{\Psi}_{ref}\right)\left(\boldsymbol{\Psi}_c^T\boldsymbol{\Psi}_c\right)} \tag{12}$$

The value of MAC is a scalar quantity that varies between 0.0 and 1.0. When the MAC value is equal to 1.0, the vectors $\boldsymbol{\Psi}_{ref}$ and $\boldsymbol{\Psi}_c$ represent exactly the same eigenmode shape. However, it is difficult to provide precise values that the MAC should take in order to guarantee good results. In this work, it is accepted that a MAC value in excess of 0.9 represents highly correlated modes and a MAC value of less than 0.05 represents uncorrelated modes [18].

4-3. Optimization procedure

Figure 2 shows a flow chart of the optimization algorithm. Initially, the initial domain is discretized by graded finite elements and the design variables are defined at each node. The initial guess for design variables ρ_{TOM}^n is chosen to be the same as the initial guess for material density at nodes ρ_{TOM}^p. The proposed formulation is implemented by using MATLAB™ code.

It is used the Q4/Q4 graded finite element, which represents a two-dimensional four-node quadrilateral GFE. Each node has three degrees of freedom: two mechanics (horizontal and vertical displacements), and one electric (electrical potential). Besides each node has a design variable. A fully isoparametric formulation is implemented in the sense that the same bilinear shape functions are applied to interpolate the unknown displacements and electric potentials, the geometry, and the material properties. In this work, the mathematical programming method (PLS) is applied to solve the linear programming [19]. It consists of the sequential solution of approximation linear sub-problems that can be defined by writing a Taylor series expansion for the non-linear optimization problem; see Eq.(7), around the current design point ρ_{TOM}^n at each iteration step. This linearization requires the sensitivities (gradients) of the objective function and constrains in relation to ρ_{TOM}^n and ρ_{TOM}^p, see Appendix.

When the eigenmode tracking is selected, the objective eigenvectors are calculated first, and then the sensitivity analysis is carried on those selected eigenvectors. Accordingly, the MAC values are calculated by comparing (see Eq.(12)) the user-defined target mode shape with those obtained by solving the eigenproblem of Eq.(3), at each iteration. Then, the eigenvectors having the MAC value closest to 1 are selected as the objective mode shapes. When the current shapes substantially change during the optimization process, the reference mode shape may be updated.

In addition, at each iteration, moving limits are defined for the design variables ρ_{TOM}^n. Typically, during the iterative process, the design variables will be allowed change by 5–15% of the original values. After linear optimization, a new set of design variables ρ_{TOM}^n and material density ρ_{TOM}^p are obtained and updated in the design domain until convergence is achieved for the

objective function. The procedure has converged when the changes in design variables from iteration to iteration are below then 10^{-3}. The final material distribution is found by projecting the design variables onto material densities layer. The finite element analysis used to obtain the response fields (electrical potentials and displacements) is based only on this projected material distribution.

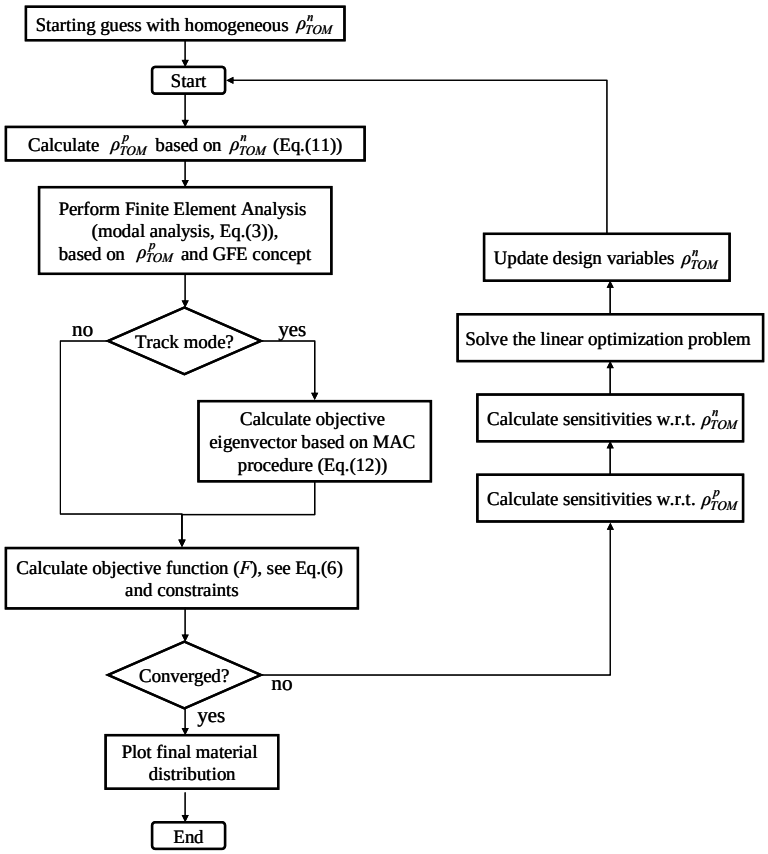

Figure 2. Flow chart of the optimization procedure.

5. RESULTS

To illustrate the proposed method, two-dimensional FGPR are designed considering plane strain assumption. The design domain used is shown in Fig.3(a). The design domain is specified as a 20 mm by 5 mm rectangle with two fixed support at the end of the left and right-hand side. The idea is simultaneously to distribute two types of materials into design domain. The material *type 1* is represented for a PZT-5A piezoelectric ceramic and the material *type 2* is a piezoelectric material PZT-5H. Initially, the design domain contains only PZT-5A material and material gradation along thickness direction is assumed. A mesh of 50 x 30 finite elements is adopted (31 layers along thickness direction), which always represent 11 and 27 nodes per wavelength on thickness and longitudinal directions.

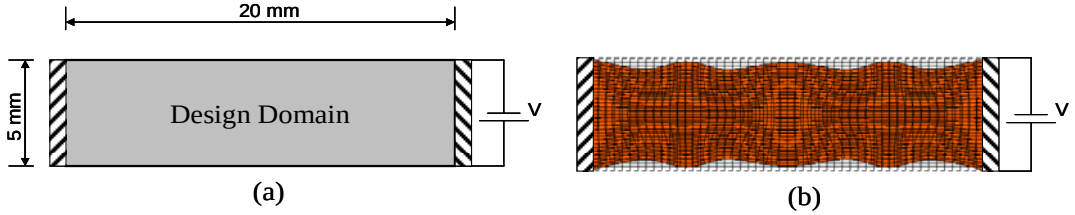

Figure 3. (a) Design domain for FGPR design. (b) Initial mode shape (dashed and solid line respectively depict non-deformed and deformed structure).

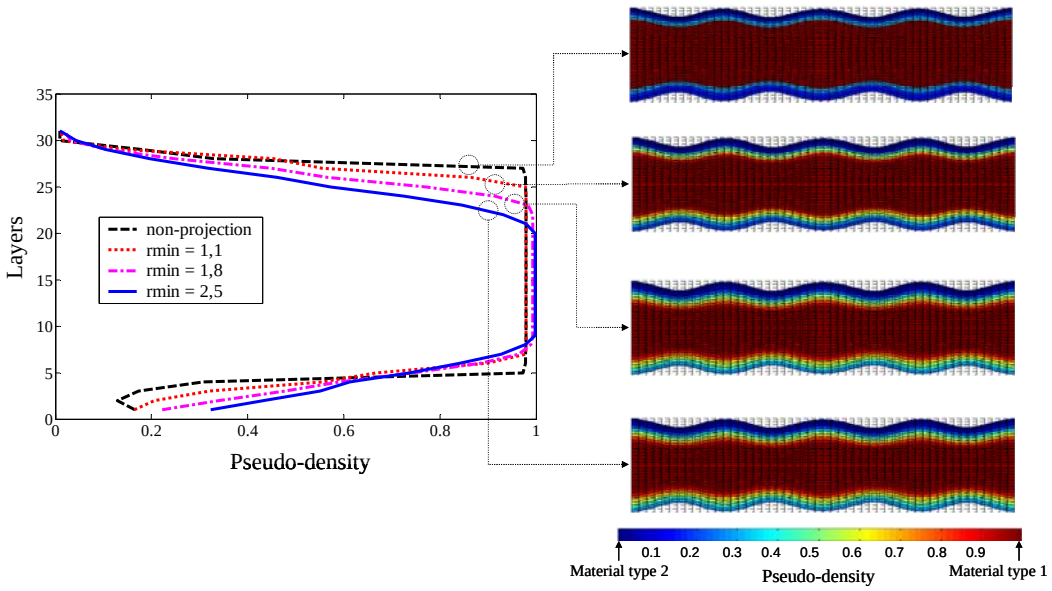

Figure 4. Final material distribution function and final mode shapes found when objective function F_3 is maximized and several r_{min} in equation (11).

In the first example, the PMC of a user-defined vibration mode shape is maximized. The reference thickness extensional mode (target mode) to be tracking along iterative optimization process is shown in Fig. 3(b) (deformed and non-deformed structure); in other word, the PMC of the piston-like mode (mode number 23) must be maximized.

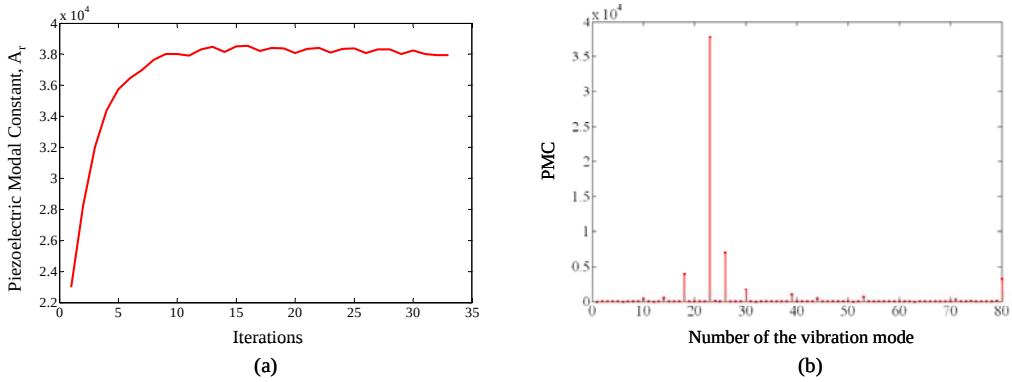

Figure 5. (a) PMC convergence history. (b) First eighty normalized PMCs.

Figure 4 shows the final material distribution law (to maximize the PMC when the FGPT vibrates in the thickness extensional mode (piston-like mode)) and the vibration mode shapes when several r_{min} in Eq. (12) are used; specifically, Fig. 4 depicts the gradation functions when non-projection technique and projection technique with r_{min} equal to 1.1; 1.8; 2.5 are utilized. According to r_{min} is incremented smother gradation functions are obtained, since the sub-domain S_i is incremented. On the other hand, Fig. 4 shows that in all simulated cases the obtained mode shape is highly correlated with initial mode shape (see Fig. 3(b)), and the final material distribution of the FGPT represents a piezoelectric transducer with only PZT-5A properties, but with PZT-5H property regions on the top and bottom surfaces. The result shows the advantage of using FGM concept and TOM to design piezoelectric transducers with maximized PMC. Particularly, when an r_{min} equal to 1.8 is used, the material distribution found increases the desirable PMC by 65.0%, from 2.299 x 10^4 to 3.794 x 10^4 (see Fig. 5(a)). In other words, the strength of the like-piston mode is increased by 65.0% when a voltage is applied across the electrodes of the FGPT, in relation to initial non-FGPT (with only PZT-5A properties). Figure 5(b) confirms that result. Figure 5(b) shows the PMC of first eighty

modes (including elastic and piezoelectric modes) of the topology optimized FGPT. The PMC of the desirable piston-like mode (mode number 23) is highest of all; thus, the optimized PMC is 880.2% and 440.7% higher than modes number 18 and 26 (adjacent modes), respectively. That dynamical behavior represents a uni-modal FGPT.

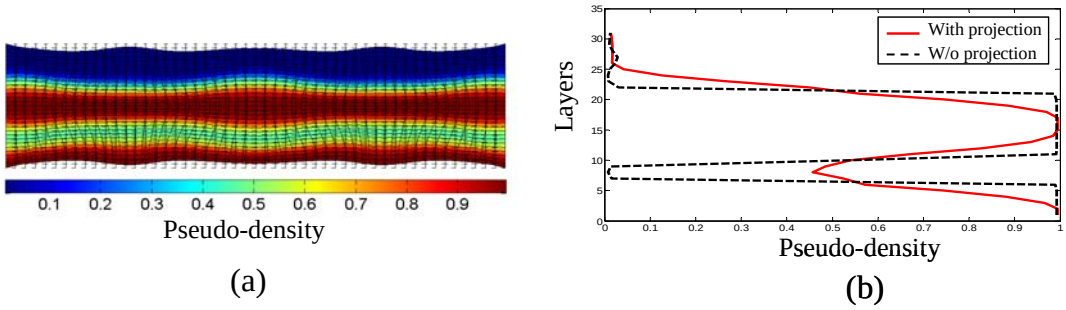

Figure 6. (a) Final mode shape. (b) Final material distribution function.

In the second example is designed a TPGF with multi-modal behavior keeping the piston-like mode of Fig. 3(b); thus, the PMC of the reference thickness extensional mode is maximized initial mode number 23) together with the left and right adjacent piezoelectric modes (mode 19 and 25, respectively). Hence, three terms at multi-objective function of Eq. (6) are utilized (m = 3). The other data are equal to example one.

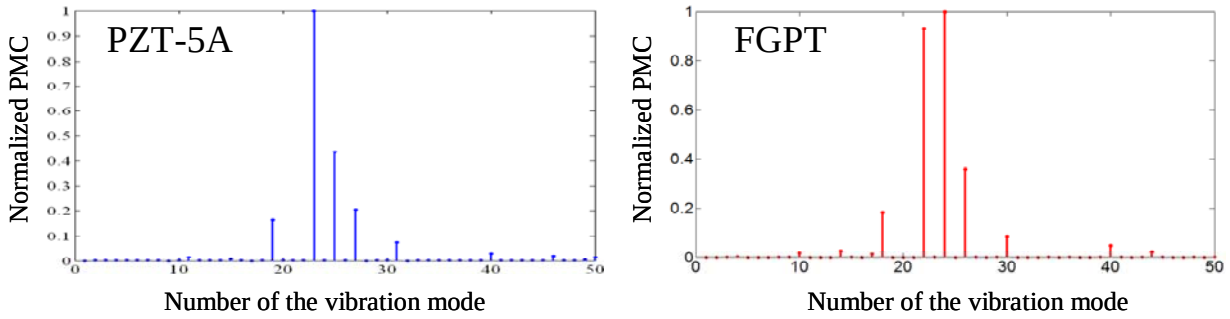

Figure 7. First fifty normalized PMCs for (a) non-FGPT and (b) topology optimized FGPT.

Figure 6(a) shows the final topology after optimization process for m = 2. This mode is a thickness extensional mode close to piston-like mode; thus, the final mode shape is very close to the initial and desirable one (see Fig. 3(b)). On the other hand, Fig. 6(b) shows the final material distribution. The projection technique leads to a more smooth material distribution. When the projection technique is not used, the optimization algorithm tends to obtain a material gradation with high property gradients, almost close to a 0 – 1 design, which is opposite to FGM concept, where smooth and continuous gradations are desired. The final material distribution depicts a Functionally Graded Piezoelectric Transducer with PZT-5A material on the bottom surface and in the middle and PZT-5H material on the top surface. In addition, from Fig. 7 is evident that the final TPGF has a bi-modal dynamic behavior with relation to non-FGPT (transducer with only PZT-5A properties). Specifically, the final modes number 22 and 24 are predominant in the total response of the transducer. The PMC of the piston-like mode was incremented 10.20%, the adjacent PMC at left was incremented by 121.51%, and the adjacent PMC at right was incremented by 10.73%.

6. CONCLUSIONS

This paper presents a systematic study of the topology optimized design of FGPT aiming to

modify their dynamic performance. The FGPT are designed using a continuum topology optimization algorithm based on: (i) a GFE to model the material gradation inside each finite element; (ii) CAMD approach to model a continuous design variable change; (iii) an explicit gradient control; (iv) a like-layer optimization problem, where the design variables are considered equals at each interfacial layer; and (v) a Modal Assurance Criterion (MAC) to track a user-defined mode shape. The TOM allows finding the optimal gradation of FGPT properties to enhance their performance in terms of user-defined PMC. The following conclusions can be drawn from these studies:

1. The topology optimization method can be successfully applied as systematic tool to design FGPT; specifically, TOM can be applied to find optimal gradation function aiming to maximize the PMC of user-defined eigenmodes.
2. The projection technique helps to find smooth gradation function which is desired for manufacturing purposes. In addition, the manufacturing of FGPT becomes possible by implementing the like-layer optimization problem; for instance, piezoelectric graded ceramics composed of green sheets can be sintering by using the Spark Plasma Sintering technique [20].
3. The Modal Assurance Criterion (MAC) arises as an adequate technique for following desired eigenmodes. This is important to design FGPT for wave generation applications, where the piston-like mode is desired, since this mode is associated with high Piezoelectric Modal Constant.
4. The numerical examples demonstrate that TOM and FGM concept can increase the Piezoelectric Modal Constant of user-defined modes. Thus, FGPT with optimal graded properties along thickness direction exhibit increment higher than 60% at first example, and higher than 120% at second example.
5. The FGPT transducers here designed can be used for designing ultrasonic FGPT with high sensibility and broadband. Generally speaking, that kind of FGPT will allow deep penetration into a specific medium (e.g. human tissues) due to its high Piezoelectric Modal Constant at specific modes, and it will produce high resolution images due to length of its frequency response (e.g. bi-modal FGPT).

ACKNOWLEDGEMENTS

The first author thanks FAPESP – São Paulo State Foundation Research Agency by supporting him in his graduate studies through the fellowship Nº. 05/01762-5. The second author is thankful for the financial support received through CNPq and FAPESP.

REFERENCES

1. Miyamoto, Y.; Kaysser, W.A.; Rabin, B.H.; Kawasaki, A.; Ford, R.G. Functionally graded materials: Design, processing and applications. Kluwer Academic Publishers, Dordrecht, (1999).
2. Wang, B.L.; Noda, N. “Design of a smart functionally graded thermopiezoelectric composite structure”. *Smart Material Structure*, Vol. 10, pp. 189-193, (2001).
3. Qui, J.; Tani, J.; Ueno, T.; Morita, T.; Takahashi, H.; Du, H. “Fabrication and high durability of functionally graded piezoelectric bending actuators”. *Smart Materials and Structures*, Vol. 12, pp. 115-121, (2003).
4. Guo, H.; Cannata, J.; Zhou, Q.; Shung, K. “Design and fabrication of broadband graded ultrasonic transducers with rectangular kerfs”. *IEEE Transaction on Ultrasonics, Ferroelectrics, and frequency Control*, Vol. 52, pp. 2096-2102, (2005).
5. Kruusing, A. “Analysis and optimization of loaded cantilever beam microactuators”. *Smart Materials and Structures*, Vol. 9, pp. 186-196, (2000).
6. Hauke, T.; Kouvatov, A.; Steinhausen, R.; Seifert, W.; Beige, H.; Langhammer, H.T.; Abicht, H. “Bending behavior of functionally graded materials”. *Ferroelectrics*, Vol.238, pp.195-202, (2000).

7. Yang, J.; Xiang, H.J. “Thermo-electro-mechanical characteristics of functionally graded piezoelectric actuators”. *Smart Materials and Structures*, Vol. 16, pp. 784-797, (2007).
8. Zhong, Z.; Yu, T. “Vibration of a simply supported functionally graded piezoelectric rectangular plate”. *Smart Materials and Structures*, Vol. 15, pp. 1404–1412, (2006).
9. Almajid, A.; Taya, M.; Hudnut, S. “Analysis of out-of-plane displacement and stress field in a piezocomposite plate with functionally graded microstructure”. *International Journal of Solids and Structures*, Vol. 38, pp. 3377-3391, (2001).
10. Kim, J.K.; Paulino, G.H. “Isoparametric graded finite elements for nonhomogeneous isotropic and orthotropic materials”. *ASME Journal of Applied Mechanics*, Vol. 69, pp. 502-514, (2002).
11. Carbonari, R.C.; Silva, E.C.N.; Paulino, G.H. “Topology optimization design of functionally graded bimorph-type piezoelectric actuators”. *Smart Materials and Structures*, Vol. 16, pp. 2607-2620, (2007).
12. Guo, N.; Cawley, P. “Measurement and prediction of the frequency spectrum of piezoelectric disks by modal analysis”. *J. Acoust. Soc. Am.*, Vol. 92, pp. 3379-3388, (1992).
13. Kim, T.S.; Kim, Y.Y. “Mac-based mode-tracking in structural topology optimization”. *Computers and Structures*, Vol. 74, pp. 375-383, (2000).
14. Matsui, K.; Terada, K. “Continuous approximation of material distribution for topology optimization”. *International Journal for Numerical Methods in Engineering*, Vol. 59, pp. 1925-1944, (2004).
15. Bendsøe, M.P.; Sigmund, O. Topology Optimization – Theory, Methods and Applications. Springer, Berlin, Heidelberg, (2003).
16. Le, C.H. Achieving minimum scale and design constraints in topology optimization: a new approach. Master thesis, University of Illinois at Urbana-Champaign, (2006).
17. Naillon, M.; Coursant, R.H.; Besnier, F. Analysis of piezoelectric structures by a finite element method. *Acta Electronica*, Vol. 25, pp. 341-362, (1983).
18. Ewins. D.J. Modal testing: theory and practice. Research Studies Pres*s*, England, (1988).
19. Haftka, R.T.; Gürdal, Z.; Kamat, M.P. Element of structural optimization. Kluwer Academic Publishers, (1990).
20. Munir, Z. A.; Anselmi-Tamburini, U.; Ohyanagi, M. “The effect of electric field and pressure on the synthesis and consolidation of materials: A review of the spark plasma sintering method”. *Journal of Materials Science*, Vol. 41, pp. 763–777, (2006).

APPENDIX

When the SLP procedure is implemented, the sensitivities of objective function (*F*) and constraints with respect to design variables are required. Basically, *F* can be considered as a function of nodal densities ρ^{p}_{TOM}, which are again a function of design variables ρ^{n}_{TOM}; thus [16]:

$$F \equiv F\left(\rho^{p}_{TOM}\left(\rho^{n}_{TOM}\right)\right) \tag{13}$$

where the variation of the function *F* is calculated as:

$$\partial F\left(\rho^{p}_{TOM}\left(\rho^{n}_{TOM\,i}\right), \partial\rho^{p}_{TOM\,i}\left(\rho^{n}_{TOM\,i}, \partial\rho^{n}_{TOM\,i}\right)\right) = \sum_{k\in S}\frac{\partial F}{\partial \rho^{p}_{TOM\,i}}\delta\rho^{p}_{TOM\,k} = \sum_{j\in S_i}\frac{\partial F}{\partial \rho^{p}_{TOM\,j}}\delta\rho^{n}_{TOM\,i} \tag{14}$$

$$\partial F\left(\rho^{p}_{TOM}\left(\rho^{n}_{TOM\,i}\right), \partial\rho^{p}_{TOM\,i}\left(\rho^{n}_{TOM\,i}, \partial\rho^{n}_{TOM\,i}\right)\right) = \left(\sum_{j\in S_i}\frac{\partial F}{\partial \rho^{p}_{TOM\,j}}\right)\delta\rho^{n}_{TOM\,i} \tag{15}$$

Thus, the variation of $\rho^{n}_{TOM\,i}$ causes the variation of a number of nodal densities, which belong

to the influence set S_i as follows:

$$\delta\rho^{\,p}_{TOM\ j}\left(\rho^{\,n}_{TOM\ i},\delta\rho^{\,n}_{TOM\ i}\right)=\begin{cases}\delta\rho^{\,n}_{TOM\ i} & for\ j\in S_i\\ 0 & otherwise\end{cases} \tag{16}$$

where S_i corresponds to the circle with its center located at the node i and radius equal to r_{min}, according to projection technique. Hence, the sensitivity of objective function F, with respect to design variable $\rho^{\,n}_{TOM\ i}$ of the node i, is expressed as:

$$\frac{\partial F}{\partial \rho^{n}_{TOM\,i}}=\sum_{j\in S_i}\frac{\partial F}{\partial \rho^{p}_{TOM\,i}} \tag{17}$$

The sensitivity of objective function F with relation to pseudo-densities $\rho^{\,p}_{TOM\ i}$ can be expressed as (differentiating the Eq. (6) with relation to $\rho^{\,p}_{TOM\ i}$):

$$\frac{\partial F_4}{\partial \rho^{\,p}_{TOM\ i}}=-F_4^{(1-n)}\sum_{k=1}^{m}w_k\,\frac{1}{\left(A_{r_k}\right)^{1-\mathbf{n}}}\frac{\partial A_{r_k}}{\partial \rho^{\,p}_{TOM\ i}} \tag{18}$$

To complete the sensitivity of F, the gradient of the PMC of the mode k ($\partial A_{r_k}/\partial \rho^{\,p}_{TOM\ i}$), with relation to pseudo-density $\rho^{\,p}_{TOM\ i}$ of node i, is required. This gradient is obtained by differentiating Eq. (4); thus:

$$\frac{\partial A_{r_k}}{\partial \rho^{\,p}_{TOM\ i}}=2W_{\mathbf{r_k}}\left(\frac{\partial\left\{\boldsymbol{\Psi}_{r_k}\right\}^T}{\partial \rho^{\,p}_{TOM\ i}}\begin{bmatrix}\boldsymbol{K}_{\boldsymbol{u\varphi}_p}\\ \boldsymbol{K}_{\boldsymbol{\varphi}_i\boldsymbol{\varphi}_p}\end{bmatrix}+\left\{\boldsymbol{\Psi}_{r_k}\right\}^T\frac{\partial}{\partial \rho^{\,p}_{TOM\ i}}\begin{bmatrix}\boldsymbol{K}_{\boldsymbol{u\varphi}_p}\\ \boldsymbol{K}_{\boldsymbol{\varphi}_i\boldsymbol{\varphi}_p}\end{bmatrix}\right)\left\{\boldsymbol{I}_p\right\} \tag{19}$$

where the sensitivity of the kth eigenmode $\boldsymbol{\Psi}_{r_k}$, in resonance, with respect to the ith pseudo-density $\rho^{\,p}_{TOM\ i}$ is obtained as:

$$\frac{\partial\left\{\boldsymbol{\Psi}_{r_k}\right\}}{\partial \rho^{\,p}_{TOM\ i}}=\sum_{\boldsymbol{j}=1}^{Nmode}a_{\mathbf{ijk}}\left\{\boldsymbol{\Psi}_{r_j}\right\} \tag{20}$$

where:

$$a_{\mathbf{ijk}}=\frac{\left\{\boldsymbol{\Psi}_{r_j}\right\}^T\left(\dfrac{\partial[\boldsymbol{K}]}{\partial \rho^{\,p}_{TOM\ i}}-\lambda_{\mathbf{r_k}}\dfrac{\partial[\boldsymbol{M}]}{\partial \rho^{\,p}_{TOM\ i}}\right)\left\{\boldsymbol{\Psi}_{r_k}\right\}}{\lambda_{\mathbf{r_k}}-\lambda_{\mathbf{r_j}}}\ \text{for}\ j\neq k;\qquad a_{\mathbf{ijk}}=-\frac{1}{2}\left\{\boldsymbol{\Psi}_{r_k}\right\}^T\frac{\partial[\boldsymbol{M}]}{\partial \rho^{\,p}_{TOM\ i}}\left\{\boldsymbol{\Psi}_{r_k}\right\}\ \text{for}\ j=k \tag{21}$$

and N_{mode} is an appropriate number of the eigenmodes associated with the lowest eigenvalues.